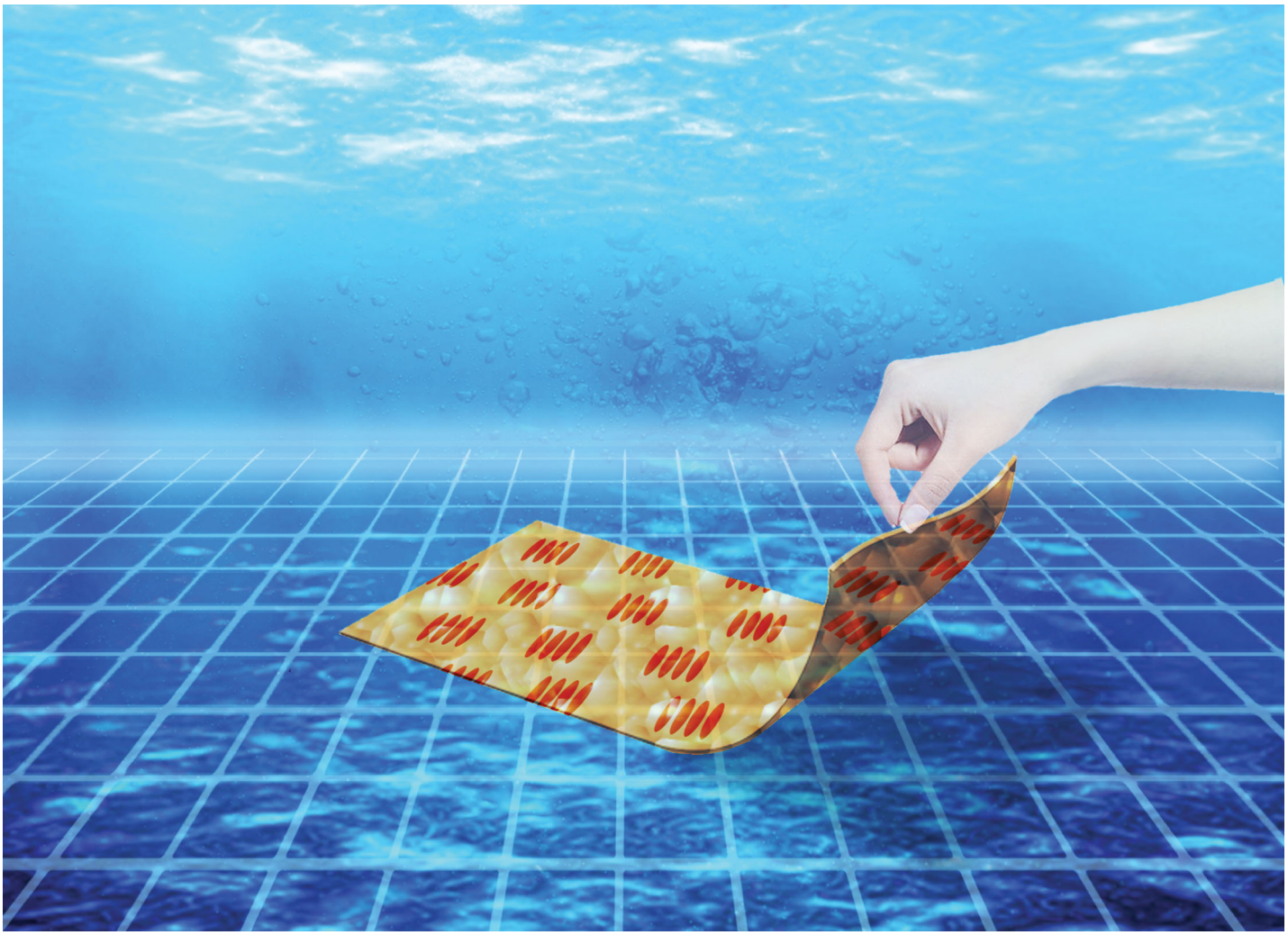

Showcasing research from the departments of Materials Science and Engineering and Biomedical Engineering at Carnegie Mellon University. Professor Christopher Bettinger is the recipient of the 2016 *Journal of Materials Chemistry* Lectureship award.

Multimodal underwater adhesion using self-assembled Dopa-bearing ABA triblock copolymer networks

Controlled radical polymerization and dopamine functionalization produce bioinspired Dopa-bearing triblock copolymers that can self-assemble into macroscopic mechanically robust networks. Dopa-rich domains (red) create physical crosslinks and domains that can improve underwater adhesion through both energy dissipation and interfacial bonding.

As featured in:

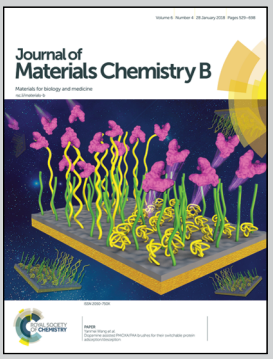

See Xiaomin Tang and Christopher J. Bettinger, *J. Mater. Chem. B*, 2018, **6**, 545.

ROYAL SOCIETY OF CHEMISTRY

rsc.li/materials-b

Registered charity number: 207890

Journal of
Materials Chemistry B

COMMUNICATION

View Article Online
View Journal | View Issue

Cite this: J. Mater. Chem. B, 2018, 6, 545

Received 4th September 2017,
Accepted 21st November 2017

DOI: 10.1039/c7tb02371e

rsc.li/materials-b

Multimodal underwater adhesion using self-assembled Dopa-bearing ABA triblock copolymer networks†

Xiaomin Tang [a] and Christopher J. Bettinger *[ab]

Self-assembled mechanically robust Dopa-bearing triblock copolymer networks improve underwater adhesion through both energy dissipation and interfacial bonding. Polymer networks that incorporate energy dissipating motifs could improve the performance of high-performance wet adhesives that only use interfacial bonds.

Underwater adhesives have many applications ranging from functional materials in marine environments to biomedical implants and coatings.[1–3] Bioinspired approaches are largely based on recapitulating the chemistry of mussel foot proteins (mfps) and have been very effective, to date.[4–7] 3,4-dihydroxyphenylalanine (Dopa) residues found in natural mfps increase the interfacial adhesion to many substrate materials by forming coordination bonds, hydrogen bonds and π–π stacking.[8–11] More recently, cation–π interactions between Dopa residues and amine groups in flanking amino acid residues in mfps can also improve adhesion by enhancing interfacial bonding.[7] Dopa residues and synergistic adhesion-promoting components can be incorporated as pendant groups or end groups in synthetic polymers to create underwater adhesives.[12–16] Despite biomimetic chemistry, there are large gaps in performance between synthetic polymers and natural mfps in terms of interfacial adhesion and toughness.[11,17,18] Dopa groups in mfps also form reconfigurable bonds that approximate the strength of covalent networks. Transient intra- and inter-molecular bonding can dissipate energy and improve the mechanical toughness in both natural[17,19,20] and synthetic adhesives.[21–24] Synthetic Dopa-bearing hydrogel networks with reconfigurable coordination bonds exhibit self-healing properties.[25] However, there are few, if any, synthetic underwater adhesives that improve performance by using reconfigurable bonds.[26–30]

Here we describe the synthesis and characterization of Dopa-bearing ABA triblock copolymers that can self-assemble into mechanically robust networks. We posit that catechol groups in Dopa molecules confer adhesive properties by promoting interfacial bonding and increasing energy dissipation through several modes of intra- and inter-molecular interactions.

The synthesis of ABA triblock copolymers is shown in Fig. 1. Poly(ethylene glycol)-based (PEG) macroinitiators are first extended with an active esterified methacrylic acid (methacrylic acid *N*-hydroxysuccinimide ester; NHSMA) by atom transfer radical polymerization (ATRP) to obtain poly(NHSMA)-*b*-PEG-*b*-poly(NHSMA) (ABA-Dopa(−)). ABA-Dopa(−) triblock copolymers are then conjugated with dopamine to produce poly(NHSMA)-*b*-PEG-*b*-poly(NHSMA)-Dopa (ABA-Dopa(+)). The resulting triblock copolymers exhibit immiscible A and B blocks, which can produce physical crosslinked networks *via* microphase separation.[31,32] Monodisperse macroinitiators combined with precise radical polymerization afforded by ATRP permit fine control over the degree of polymerization (DP) of network precursors (poly-(NHSMA)$_{70}$-*b*-PEG$_{228}$-*b*-poly(NHSMA)$_{70}$; A$_{70}$B$_{228}$A$_{70}$). Furthermore, amine-reactive NHSMA can support a Dopa conjugation ratio approaching 70% on a NHSMA monomer basis as calculated by ^{1}H NMR and supported by UV-vis spectroscopy (see Fig. S2, S4 and S5, ESI†). A$_{70}$B$_{228}$A$_{70}$ triblocks with the nominal Dopa conjugation ratio of 70% were chosen for subsequent network formation studies because the role of Dopa groups could be best elucidated with the maximum concentration of Dopa in phases rich in A segments of the ABA triblock copolymers.

Self-assembled polymer networks were prepared from both ABA-Dopa(−) and ABA-Dopa(+) polymer precursors. Concentrated polymer solutions in *N*,*N*-dimethylformamide (DMF) were first cast into films and then assembled into networks through phase separation by solvent exchange with excess water. The solvent exchange disrupts crystalline PEG domains as assessed by differential scanning calorimetry (DSC; Fig. S6, ESI†). We posit that the solvent exchange process generates phases rich in A blocks that serve as physical crosslinks and are joined together by PEG-based B blocks. Mechanically robust networks can be produced through solvent exchange using precursors with B blocks of MW_{PEG} = 10 000 g mol^{-1} (DP_{PEG} = 228). Precursors of B blocks

[a] Department of Materials Science and Engineering, Carnegie Mellon University, Pittsburgh, PA 15213, USA. E-mail: cbetting@andrew.cmu.edu
[b] Department of Biomedical Engineering, Carnegie Mellon University, Pittsburgh, PA 15213, USA

† Electronic supplementary information (ESI) available. See DOI: 10.1039/c7tb02371e

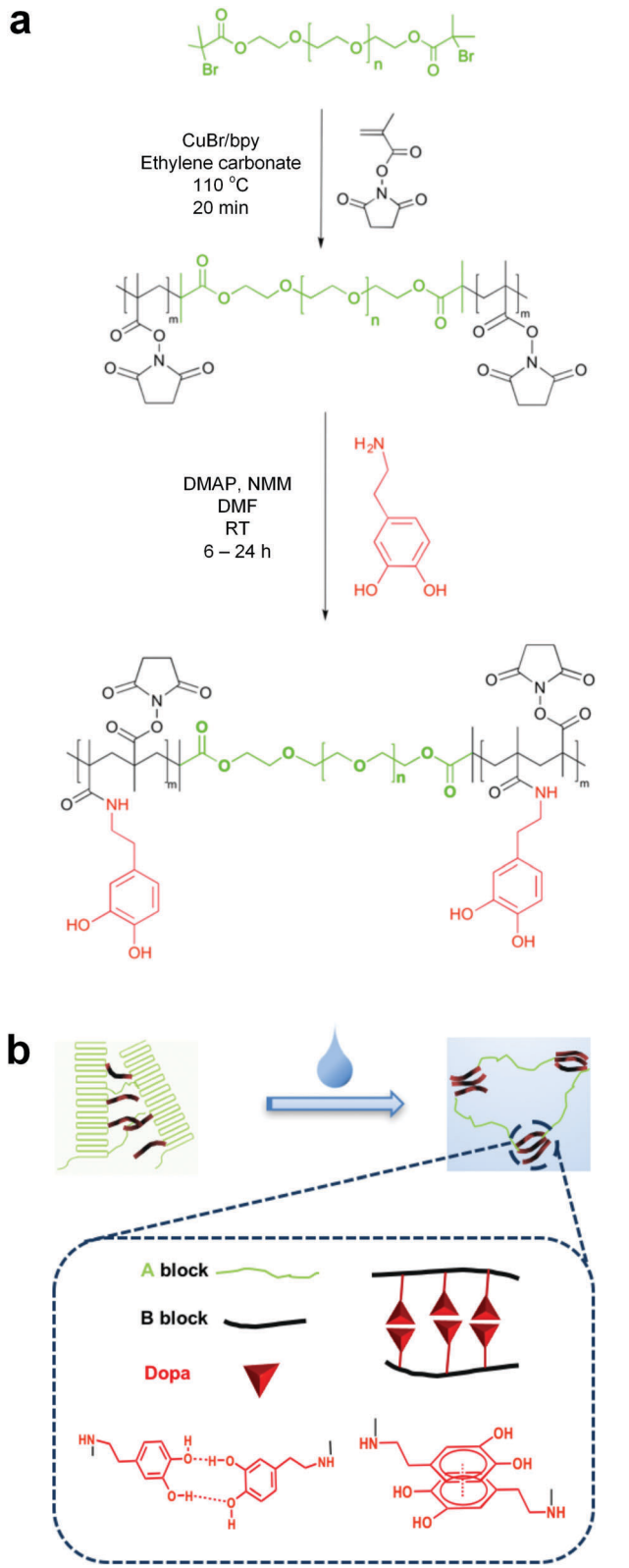

Fig. 1 Design and processing of precursor. (a) Schematic showing the synthesis of poly(NHSMA)-*b*-PEG-*b*-poly(NHSMA) (ABA-Dopa(−)) and poly(NHSMA)-*b*-PEG-*b*-poly(NHSMA)-Dopa (ABA-Dopa(+)) triblock copolymers. (b) Schematic illustration of polymer processing to create the hydrated ABA-Dopa(+) network.

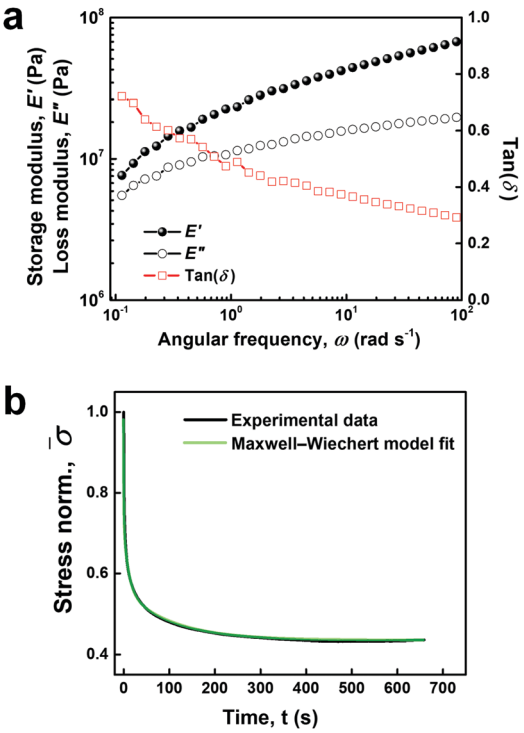

Fig. 2 Viscoelastic properties of ABA-Dopa(+) networks comparison to linear viscoelastic models. (a) Storage (E') and loss (E'') modulus are plotted as a function of angular frequency obtained from tensile oscillatory sweeps (ε = 0.5%; ω = 0.1–100 rad s^{-1}). (b) Plots of stress relaxation curves for both experimental data and fitting curve using Maxwell–Wiechert model (inset).

of DP_{PEG} = 450 and DP_{PEG} = 92 create brittle networks and therefore the mechanical properties were not investigated further in this study. The former may be caused by excess PEG crystallization and the later may be attributed to excessive loop formation. The length of the B block is therefore critical in realizing mechanically robust adhesive polymer networks.

Dynamic mechanical analysis (DMA) was performed on both ABA-Dopa(−) and ABA-Dopa(+) films. Networks prepared from ABA-Dopa(+) triblock copolymers exhibit solid-like behavior with a storage modulus of $E' \sim 10^7$ Pa that monotonically increases for ω = 0.1–100 rad s^{-1}. The storage modulus is orders of magnitude larger than other types of hydrated catechol-bearing networks (Table S5, ESI†).[33,34] Strikingly, the loss modulus E'' of ABA-Dopa(+) networks, which is 5 times larger than the E'' of ABA-Dopa(−) networks, possesses the same order with E'. In addition, the markedly increased tan(δ) suggests that ABA-Dopa(+) networks have a larger viscosity compared to ABA-Dopa(−) films. The differential mechanical properties are attributed to dynamic interactions between Dopa motifs in phases rich in A blocks. The loss modulus of ABA-Dopa(+) networks increases from E'' = 5 to 10 MPa over ω = 0.1–100 rad s^{-1} whereas the loss modulus of ABA-Dopa(−) networks is largely constant at E'' = 1–2 MPa in the same frequency range. The value of E'' in ABA-Dopa(+) networks increases monotonically with frequency, which suggests multiple dissipation processes are present and span time scales across several orders of magnitude. Rapid dissipation processes at high frequencies are present in ABA-Dopa(+) networks

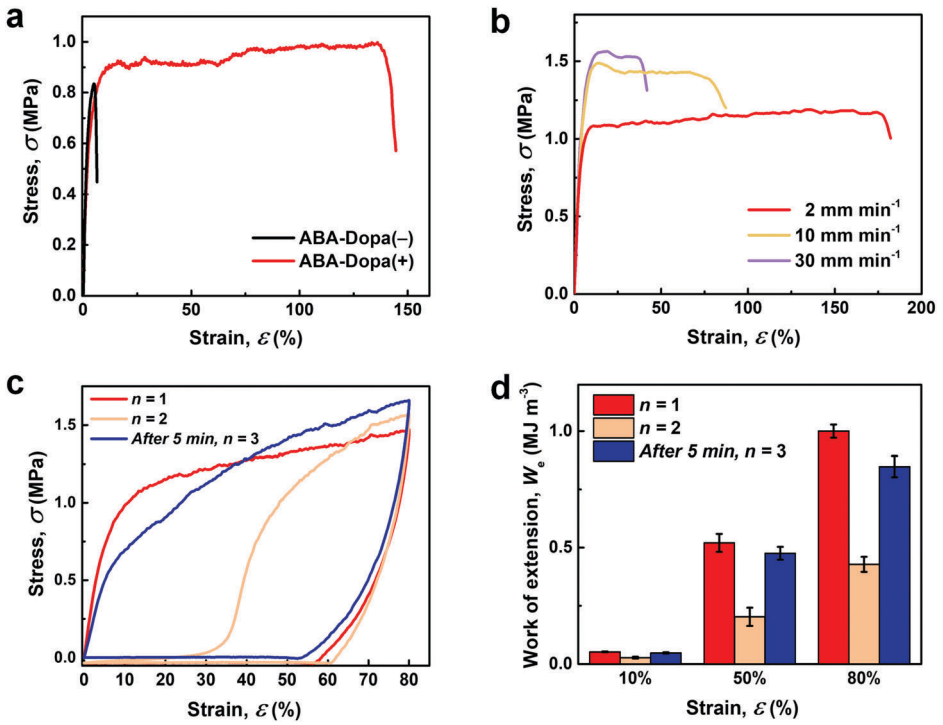

Fig. 3 Mechanical properties of networks. (a) Tensile test results for networks prepared from ABA-Dopa(–) and ABA-Dopa(+) triblock copolymer precursors at a strain rate of 2 mm min^{-1} (see Experimental methods for details). (b) Stress–strain curves of networks prepared from ABA-Dopa(+) as a function of strain rate. (c) Cyclic tensile curves of films prepared from ABA-Dopa(+) at a nominal strain of ε = 80%: first loading–unloading cycle (n = 1, red); successive stretching curve (n = 2, orange); cycle after 5 min rest (*after 5 min*, n = 3, blue). (d) Work of extension of films at nominal strains of ε = 10%, 50%, and 80% for n = 1, 2, and 3 (*after 5 min*), respectively.

and typically associated with reconfigurable bonds.[35,36] The solid-like, yet viscous behavior of this material is attributed to intra- and inter-molecular interactions of Dopa within phases rich in A blocks.

The viscoelastic properties of networks composed of ABA-Dopa(+) polymers were further studied using stress relaxation measurements and modeled using a Maxwell–Wiechert linear viscoelastic model (Fig. 2b). The best fit for the Maxwell–Wiechert model was achieved using the following four elements in parallel: three Maxwell elements plus an additional elastic element. The relaxation times of each corresponding Maxwell element are 0.76 ± 0.009, 9.87 ± 1.48, and 114.28 ± 11.91 s, respectively. These relaxation modes span three orders of magnitude and are associated with multiple dissipation processes from Dopa interactions concentrated in phases rich in A blocks and PEG bridges rich in B blocks. H-Bonding in polymer networks exhibits a characteristic relaxation time of 3–6 s.[37] Based on the relation between relaxation time τ and bond energy E_a given by $\tau \propto e^{E_a/RT}$, the relaxation time of 0.76 s is consistent with dissipation due to π–π interactions. Relatively longer relaxation time scale could be related to the dissociation of H-bonding clusters or entanglements in PEG chains.[38,39]

Pendant Dopa residues improve the mechanical toughness and resilience of ABA triblock copolymer networks. The tensile properties of both ABA-Dopa(–) and ABA-Dopa(+) networks are shown in Fig. 3a. The Young's moduli of films composed of ABA-Dopa(+) and ABA-Dopa(–) polymers are $E_{\text{ABA-Dopa(+)}}$ = 32 ± 4.7 MPa

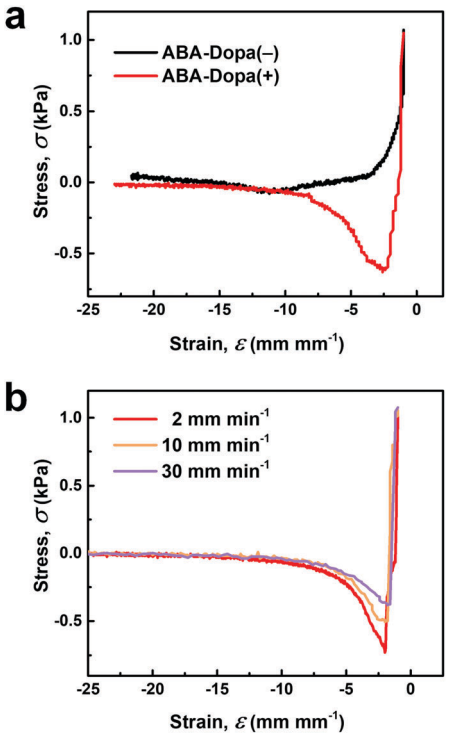

Fig. 4 Wet adhesion properties of ABA triblock copolymer networks. (a) Stress–strain curves extracted from force–distance curves between glass probes and substrates composed of networks prepared from ABA-Dopa(–) and ABA-Dopa(+) polymers. (b) Stress–strain curves for ABA-Dopa(+) networks performed at different retraction rates.

Table 1 Summary of relevant mechanical and adhesive properties in ABA-Dopa(−) and ABA-Dopa(+) networks

Sample	Dopa ratio[a] (%)	Storage modulus, E' (Pa)	Loss modulus, E'' (Pa)	Toughness, W_e (MJ m^{-3})	Work of adhesion, W_{ad} (J m^{-2})
ABA-Dopa(+)	70	$(0.7–8) \times 10^7$	$(0.55–1) \times 10^7$	1.55 ± 0.43	0.12 ± 0.01
ABA-Dopa(−)	0	$(2–4) \times 10^7$	$(0.1–0.2) \times 10^6$	0.025 ± 0.021	0[b]

[a] Dopa ratio (%) indicates the mole fraction of the Dopa conjugated A block in the total A block. [b] Below the detection limit of our instrumentation and methods.

and $E_{\text{ABA-Dopa(−)}} = 28 \pm 2.8$ MPa, respectively. Although the Young's moduli are comparable, the tensile toughness and maximum elongation are greatly increased in networks composed of ABA-Dopa(+) polymers (Table S2, ESI†). Networks prepared from ABA-Dopa(+) polymers exhibit rate-dependent tensile toughness, values for maximum elongation and breaking stress (Fig. 3b and Table S2, ESI†). This behavior has been observed previously in crosslinked networks that contain reconfigurable H-bonds and ionic crosslinks.[38,40] We anticipate that reconfigurable transient bonds in phases rich in A blocks produce a cycle-dependent toughness (Fig. 3c). The strain energy dissipated reduces larger than half from the first cycle to the second cycle. If a recovery time of 5 min is permitted, the strain energy dissipated in the second cycle is increased substantially (Fig. 3d and Table S3, ESI†). The observed time-dependent recovery of energy dissipation is attributed to the reformation of transient intra- and inter-molecular bonds between Dopa groups in physical crosslinks rich in A blocks.

Dopa groups increase underwater adhesion in polymers by enhancing interfacial bonding and increasing the energy dissipation capacity within the polymer network. Physically crosslinked polymer networks prepared from ABA-Dopa(−) polymers exhibit limited adhesion compared to polymer networks prepared from ABA-Dopa(+). These results suggest that catechol groups increase interfacial adhesion in hydrated conditions even if they are embedded in phases rich in A blocks (Fig. 4a). The work of adhesion in wet environments for ABA-Dopa(+) is also a strong function of the retraction rate of the probe (Fig. 4b and Table S4, ESI†), an observation that is consistent with the tensile rate-dependent toughness. ABA-Dopa(+) networks exhibit broad relaxation times ranging from 0.76 to 114 s. A force–distance measurement with a retraction velocity of 2 mm min^{-1} rate requires 450 s to complete. This time scale permits all observed dissipation modes to occur. Conversely, force–distance measurements using retraction velocities of 10 mm min^{-1} and 30 mm min^{-1} (requiring 90 and 30 s to complete, respectively) restrict some dissipation modes and therefore produce smaller values for the calculated work of adhesion. We infer that networks prepared from ABA-Dopa(+) triblock polymers enhance underwater adhesion by increasing the areal density of interfacial bonds and creating dissipative networks in physical crosslinks composed of phases rich in Dopa-bearing A blocks.

We have designed and synthesized networks composed of Dopa-bearing self-assembled ABA triblocks with the following characteristic mechanical properties: a Young's modulus of $E \sim 28$ MPa; an ultimate tensile stress of $\sigma_b \sim 1.1$ MPa; and a maximum elongation at break of $\varepsilon_{max} \sim 130\%$ (Table S2, ESI†). ABA-Dopa(+) triblock polymers form mechanically resilient networks that exhibit adhesion in hydrated conditions. Compared to ABA-Dopa(−) films, Dopa-bearing polymer networks promote adhesion through mechanisms including interfacial bonding and strain energy dissipation through multiple types of intra- and inter-molecular bonds (Table 1). The synthesis strategy described herein affords molecular control over the composition of network precursors by using B blocks of monodisperse telechelic macroinitiators that can be extended to create A blocks with precise DP and degree of substitution of Dopa. In addition to H-bonding and π–π interactions, it may be possible to incorporate additional energy dissipation modes through reconfigurable coordination bonding between catechols and cations to further enhance underwater adhesion. The collective chemical and mechanical properties afforded by the unique molecular design suggest that ABA-Dopa(+) triblock polymers have potential applications as functional materials for marine environments, surgical adhesives, or substrate materials for ultracompliant hydrogel-based electronic devices.[16,41]

Author contributions

C. J. B. and X. M. T. designed the synthesis scheme, methodology for characterizing the material, and wrote the manuscript. X. M. T. performed the experiments.

Conflicts of interest

The authors declare no competing financial interests.

Acknowledgements

X. M. T. thanks to the following people for the help and discussion of synthesis, dynamic mechanical test and adhesion test. They are Liye Fu, Hangjun Ding, Yi Shi, Bill Pingitore, Sipei Li and Iksoo Kwon. The authors acknowledge financial support provided by the following organizations: National Institutes of Health (R21NS095250); the Defense Advanced Research Projects Agency (D14AP00040); the National Science Foundation (DMR1542196); the Carnegie Mellon University School of Engineering. The authors would also like to thank the CMU Thermomechanical Characterization Facility in the Department of Materials Science and Engineering.

References

1 R. J. Stewart, T. C. Ransom and V. Hlady, *J. Polym. Sci., Part B: Polym. Phys.*, 2011, **49**, 757–771.
2 N. Annabi, A. Tamayol, S. R. Shin, A. M. Ghaemmaghami, N. A. Peppas and A. Khademhosseini, *Nano Today*, 2014, **9**, 574–589.

3 G. Kaplan, *Plast. Reconstr. Surg.*, 1966, **37**, 139–142.
4 B. P. Lee, P. B. Messersmith, J. N. Israelachvili and J. H. Waite, *Annu. Rev. Mater. Res.*, 2011, **41**, 99–132.
5 D. G. Barrett, G. G. Bushnell and P. B. Messersmith, *Adv. Healthcare Mater.*, 2013, **2**, 745–755.
6 H. Lee, B. P. Lee and P. B. Messersmith, *Nature*, 2007, **448**, 338–341.
7 Q. Zhao, D. W. Lee, B. K. Ahn, S. Seo, Y. Kaufman, J. N. Israelachvili and J. H. Waite, *Nat. Mater.*, 2016, **15**, 407–412.
8 H. Lee, N. F. Scherer and P. B. Messersmith, *Proc. Natl. Acad. Sci. U. S. A.*, 2006, **103**, 12999–13003.
9 T. Utzig, P. Stock and M. Valtiner, *Angew. Chem., Int. Ed.*, 2016, **55**, 9523–9527.
10 Q. Ye, F. Zhou and W. Liu, *Chem. Soc. Rev.*, 2011, **40**, 4244–4258.
11 H. G. Silverman and F. F. Roberto, *Mar. Biotechnol.*, 2007, **9**, 661–681.
12 C. R. Matos-Perez, J. D. White and J. J. Wilker, *J. Am. Chem. Soc.*, 2012, **134**, 9498–9505.
13 M. A. North, C. A. Del Grosso and J. J. Wilker, *ACS Appl. Mater. Interfaces*, 2017, **9**, 7866–7872.
14 C. E. Brubaker, H. Kissler, L. J. Wang, D. B. Kaufman and P. B. Messersmith, *Biomaterials*, 2010, **31**, 420–427.
15 B. P. Lee, J. L. Dalsin and P. B. Messersmith, *Biomacromolecules*, 2002, **3**, 1038–1047.
16 H. Wu, V. Sariola, C. Zhu, J. Zhao, M. Sitti and C. J. Bettinger, *Adv. Mater.*, 2015, **27**, 3398–3404.
17 J. J. Wilker, *Science*, 2015, **349**, 582–583.
18 J. H. Waite, N. H. Andersen, S. Jewhurst and C. J. Sun, *J. Adhes.*, 2005, **81**, 297–317.
19 D. S. Hwang, M. J. Harrington, Q. Y. Lu, A. Masic, H. B. Zeng and J. H. Waite, *J. Mater. Chem.*, 2012, **22**, 15530–15533.
20 S. Kim, A. Faghihnejad, Y. Lee, Y. Jho, H. Zeng and D. S. Hwang, *J. Mater. Chem. B*, 2015, **3**, 738–743.
21 X. H. Zhao, *Soft Matter*, 2014, **10**, 672–687.
22 S. C. Grindy, R. Learsch, D. Mozhdehi, J. Cheng, D. G. Barrett, Z. B. Guan, P. B. Messersmith and N. Holten-Andersen, *Nat. Mater.*, 2015, **14**, 1210–1216.
23 T. L. Sun, T. Kurokawa, S. Kuroda, A. Bin Ihsan, T. Akasaki, K. Sato, M. A. Haque, T. Nakajima and J. P. Gong, *Nat. Mater.*, 2013, **12**, 932–937.
24 N. Holten-Andersen, A. Jaishankar, M. J. Harrington, D. E. Fullenkamp, G. DiMarco, L. H. He, G. H. McKinley, P. B. Messersmith and K. Y. C. Leei, *J. Mater. Chem. B*, 2014, **2**, 2467–2472.
25 N. Holten-Andersen, M. J. Harrington, H. Birkedal, B. P. Lee, P. B. Messersmith, K. Y. C. Lee and J. H. Waite, *Proc. Natl. Acad. Sci. U. S. A.*, 2011, **108**, 2651–2655.
26 K. R. Shull and C. Creton, *J. Polym. Sci., Part B: Polym. Phys.*, 2004, **42**, 4023–4043.
27 A. Roos and C. Creton, *Macromolecules*, 2005, **38**, 7807–7818.
28 N. Amouroux, J. Petit and L. Leger, *Langmuir*, 2001, **17**, 6510–6517.
29 A. Lindner, B. Lestriez, S. Mariot, C. Creton, T. Maevis, B. Luhmann and R. Brummer, *J. Adhes.*, 2006, **82**, 267–310.
30 J. Li, A. D. Celiz, J. Yang, Q. Yang, I. Wamala, W. Whyte, B. R. Seo, N. V. Vasilyev, J. J. Vlassak, Z. Suo and D. J. Mooney, *Science*, 2017, **357**, 378–381.
31 C. C. Zhu and C. J. Bettinger, *Macromol. Rapid Commun.*, 2013, **34**, 1446–1451.
32 C. C. Zhu and C. J. Bettinger, *Macromolecules*, 2015, **48**, 1563–1572.
33 Y. Tanaka, K. Fukao and Y. Miyamoto, *Eur. Phys. J. E: Soft Matter Biol. Phys.*, 2000, **3**, 395–401.
34 S. Naficy, H. R. Brown, J. M. Razal, G. M. Spinks and P. G. Whitten, *Aust. J. Chem.*, 2011, **64**, 1007–1025.
35 J. Y. Sun, X. H. Zhao, W. R. K. Illeperuma, O. Chaudhuri, K. H. Oh, D. J. Mooney, J. J. Vlassak and Z. G. Suo, *Nature*, 2012, **489**, 133–136.
36 T. Annable, R. Buscall, R. Ettelaie and D. Whittlestone, *J. Rheol.*, 1993, **37**, 695–726.
37 X. B. Hu, J. Zhou, W. F. M. Daniel, M. Vatankhah-Varnoosfaderani, A. V. Dobrynin and S. S. Sheiko, *Macromolecules*, 2017, **50**, 652–659.
38 X. B. Hu, M. Vatankhah-Varnoosfaderani, J. Zhou, Q. X. Li and S. S. Sheiko, *Adv. Mater.*, 2015, **27**, 6899–6905.
39 O. Chaudhuri, L. Gu, D. Klumpers, M. Darnell, S. A. Bencherif, J. C. Weaver, N. Huebsch, H. P. Lee, E. Lippens, G. N. Duda and D. J. Mooney, *Nat. Mater.*, 2016, **15**, 326–334.
40 C. H. Li, C. Wang, C. Keplinger, J. L. Zuo, L. Jin, Y. Sun, P. Zheng, Y. Cao, F. Lissel, C. Linder, X. Z. You and Z. A. Bao, *Nat. Chem.*, 2016, **8**, 619–625.
41 H. Wu, V. Sariola, J. Zhao, H. Ding, M. Sitti and C. Bettinger, *Polym. Int.*, 2016, **65**, 1355–1359.